SOURCE-RECEPTOR MODELING USING HIGH RESOLUTION WRF METEOROLOGICAL FIELDS AND THE HYSPLIT MODEL TO ASSESS MERCURY POLLUTION OVER THE MISSISSIPPI GULF COAST REGION

Anjaneyulu Yerramilli [1,*], Venkata Bhaskar Rao Dodla[1] , Hari Prasad Dasari[1] , Challa Venkata Srinivas[1], Francis Tuluri[2], Julius M. Baham[1], John H. Young[1], Robert Hughes[1], Chuck Patrick[1], Mark G. Hardy[2], Shelton J. Swanier[1], Mark.D.Cohen[3] , Winston Luke[3] , Paul Kelly[3] and Richard Artz[3]

[1] Trent Lott Geospatial Visualization Research Centre, Jackson State University, Jackson MS 39217,USA
[2]College of Science, Engineering &Technology, Jackson State University, Jackson MS 39217,USA
[3]NOAA Air Resouce Laboratory, NOAA/ARL, 1315 East WestHighway ,Silver Spring, Maryland 20910-3282, USA

ABSTRACT

The Mississippi Gulf Coastal region is environmentally sensitive due to multiple air pollution problems originating as a consequence of several developmental activities such as oil and gas refineries, operation of thermal power plants, and mobile-source pollution. Mercury is known to be a potential air pollutant in the region apart from SOX, NOX,CO and Ozone. Mercury contamination in water bodies and other ecosystems due to deposition of atmospheric mercury is considered a serious environmental concern. Identification of sources contributing for the high atmospheric mercury levels will be useful for formulating pollution control and mitigation strategies in the region.

The present study demonstrates the use of high-resolution output from the WRF (Weather Research Forecast) model as input to the HYSPLIT atmospheric dispersion model to analyze a high mercury concentration episode measured at the Grand Bay National Estuarine Research Reserve (NERR).

A high mercury concentration episode observed at the Grand Bay NERR during May 5-6, 2008 was selected as a case study. The peak concentration of reactive gaseous mercury (RGM) measured was 170 pg/m3 during this episode, an order of magnitude above the background concentrations observed at the site. The study comprises of two components, one to produce high resolution atmospheric fields (4 km) using WRF-ARW model and the other to drive the HYSPLIT dispersion model using this WRF-ARW output to generate backward trajectories from the NERR station and forward trajectories from the known elevated point sources in the region. The ARW model was used with three one-way interactive nested domains with 36-12-4 km resolutions, 43 vertical levels with the inner finest domain covering the study

The model simulated meteorological fields were used to study the diurnal variations of the atmospheric fields and the characteristics of the boundary layer over the study region and are evaluated by comparison against available meteorological observations.

The HYSPLIT atmospheric dispersion model, driven by the output from WRF model, was used to obtain the Lagrangian path of trajectories from the NERR observation station. Backward trajectories were generated for every hour during May 4-7, corresponding to the episode and for one day before and after the episode. These back trajectories are used in conjunction with a regional mercury emissions inventory to identify the potential sources of mercury contributing to the high concentrations observed. Throughout the study, trajectory results using high-resolution WRF meteorological data fields are compared with trajectories estimated using coarser meteorological data, e.g., the NOAA EDAS 40km dataset. Results from the backward trajectories and the forward dispersion simulations indicate that two sources (Charles R Lowman power plant and Barry power plant in Alabama) are likely to significantly contribute to the observed peaks of RGM at NERR location in MS Gulf coast. This study is part of a larger collaborative effort between Jackson State University, NOAA, and the Grand Bay NERR to study the dispersion of atmospheric pollutants in the Gulf Coast region.

Key Words:WRF; HYSPLIT; Simulation-$PM_{2.5}$; Source identification

1. INTRODUCTION

The growth of industrial and commercial operations near shoreline has created a need for precise air pollution dispersion models that can handle unique meteorological conditions present in the coastal environment. The Mississippi Gulf coast has a complex coastal topography. Differential heating, strong thermal gradients along the land-sea interface and topographic friction cause localized meso-scale phenomena such as land-sea breeze circulations, sea breeze induced convection and formation of thermal internal boundary layer. The horizontal and vertical extents of the land-sea breeze, the internal boundary layer and their spatial heterogeneity under varying synoptic meteorological settings typify the complex dispersion patterns in the coastal region. The Thermal Internal Boundary Layer (TIBL) especially limits the region of vertical mixing, heating/ convection and the low-level circulation characteristics which influence the coastal area dispersion. These spatio-temporal effects need to be accounted in the dispersion assessment for realistic air quality estimations using appropriate atmospheric

[*]Corresponding author E-Mail: yerramilli.anjaneyulu@jsums.edu

hydro-dynamic and dispersion models. Dispersion is influenced due to the development of mesoscale circulations as a result of differential heating of the land and water surfaces (Pielke et al 1991; Lu and Turco, 1995).

Mercury is known to be a potential air pollutant in the region apart from SOX, NOX,CO and Ozone. Mercury contamination in water bodies and other ecosystems due to deposition of atmospheric mercury is considered a serious environmental concern. Identification of sources contributing for the high atmospheric mercury levels will be useful for formulating pollution control and mitigation strategies in the region. Atmospheric forms and behavior of mercury are complex owing to its existence in both elemental (Hg/Hg(O)) and divalent / oxidized forms (Hg (Hg(II)). Several Chemistry Transport Models are currently used to simulate atmospheric mercury fate and transport. Emissions of sulfur dioxide (SO_2), volatile organic compounds (VOCs), halogen gases, and carbon-rich particulate aerosols are believed to have an important effect on chemical and physical transformations of mercury in air and in cloud water.

Mesoscale atmospheric models are widely used for complex terrain to capture the complex flow and meteorological parameters essential in dispersion estimations (Physick and Abbs, 1991; Kotroni et al., 1999; Wang et al., 2004 among others). The SO_2 concentrations from major elevated sources in Southern Florida are studied with a coupled dispersion model by Segal et al (1998) which showed that the local sea-breeze circulations lead to complex dispersion pattern leading to higher concentrations on the east coast. Moran and Pielke (1996) used a coupled mesoscale atmospheric and dispersion modeling system for tracer dispersion over complex topographic regions. Jin and Raman (1996) studied dispersion from elevated releases under the sea-land breeze flow using a mesoscale dispersion model which included the effects of local topography, variability in wind and stability. Anjaneyulu et al (2008, 2009) and Challa et al (2008, 2009) have studied the atmospheric dispersion over the Mississippi Gulf Coast region using an integrated mesoscale weather prediction and atmospheric dispersion models.

In this paper our studies on source-receptor relationships for atmospheric mercury by integrating high-resolution output from the WRF (Weather Research Forecast) model to the HYSPLIT atmospheric dispersion model to analyze a high mercury concentration episode measured at the Grand Bay National Estuarine Research Reserve (NERR) are presented. The main focus is on the development of prediction methodology for the atmospheric fields of wind, temperature, humidity, PBL turbulence; backward trajectory calculations for source identification, reverse mode dispersion calculations for source attribution and forward mode computations for ambient concentrations.

One episode of maximum in the observations of Mercury at the NERR Grand Bay observation station of NOAA, during 00 UTC of 3 May to 00 UTC of 8 May 2008.was chosen to study the impact of atmospheric flow fields on the identification of sources as well as of the dispersion characteristics.

2. MODELS, DATA AND METHODOLOGY

The meteorological fields required for the dispersion calculations are obtained through two approaches. Initially the Eta Data Assimilation (EDAS) north American regional analysis and forecasts from the NCEP are used to conduct the backward trajectory analysis and the forward dispersion simulations. EDAS is a regional analyses for North America based on the Eta regional model and data are available at 3 h intervals on Eta 212 grid at a spatial resolution of 40 km on 26 vertical levels from 1,000 mb to 50 mb. Inorder to study the impact of the high resolution meteorological data sets on the source –receptor assessment a mesoscale model is run using nested domains with suitable grid resolutions. The ARW (Advanced Research WRF) model is used to produce the atmospheric fields at a high resolution over the study region for the desired time period. This model system has versatility to choose the domain region of interest; horizontal resolution; interactive nested domains and with various options to choose parameterization schemes for convection, planetary boundary layer (PBL), explicit moisture; radiation and soil processes (Skamarock et al.2008). ARW is suitable for use in a broad range of applications across scales ranging from meters to thousands of kilometers.

The ARW model is designed with three nested grids (36, 12 and 4 km) and with 43 vertical levels. The outer domain covered the South-central US and the surrounding Atlantic Ocean (Figure 1). The inner finer grid covered the Mississippi Gulf Coast off Louisiana above the Gulf of Mexico. The model domains are centered at 32.8° N, -87.5° E with Lambert Conformal Conic (LCC) projection. The grid sizes in the east-west and north-south directions in each domain are 56x42, 109x82 and 178x136 respectively. The second and third nests are one way interactive. The model physics options used are Kain-Fritsch scheme (Kain and Fritisch, 1993) for convective parameterization, WRF Single Moment Class 3 (WSM3) simple ice scheme for explicit moisture , Yonsei University non-local scheme for boundary layer (Hong et al., 2006), standard five-layer soil model (Dudhia, 1996), Dudhia scheme for short wave radiation (1989) and the Rapid Radiative Transfer Model (Mlawer et al., 1997) for longwave radiation processes. The model is initialized at 00 UTC 4 June and integrated for 48 hours using EDAS data for initial and boundary conditions as outlined above. The USGS topography and vegetation data (25 categories) and FAO Soils data (17 categories) with resolutions 5m, 2m and 30 sec (0.925 km) were used to define the lower boundary conditions. The initial and boundary conditions required for ARW model integrations are adopted from National Centers of Environmental Prediction (NCEP) North American regional analysis and forecasts (EDAS) 40 km resolution data. The boundary conditions are updated at every 6 hour interval (i.e.) at 00, 06, 12 and

18 UTC during the period of model integration from the EDAS forecasts.

2b. *Description of Pollution Dispersion Model*

The HYSPLIT 4.9 (Hybrid Single-Particle Lagrangian Integrated Trajectory) was used for computing simple air parcel trajectories to complex dispersion and deposition simulations (Draxler and Hess, 1998). HYSPLIT computes the advection of a single pollutant particle, or simply its trajectory. The dispersion of a pollutant is calculated by assuming either puff or particle dispersion. In the puff model, puffs expand until they exceed the size of the meteorological grid cell (either horizontally or vertically) and then split into several new puffs, each with its share of the pollutant mass. In the particle model, a fixed number of initial particles are advected about the model domain by the mean wind field and a turbulent component. The model's default configuration assumes a puff distribution in the horizontal and particle dispersion in the vertical direction. In this way, the greater accuracy of the vertical dispersion parameterization of the particle model is combined with the advantage of having an ever expanding number of particles represent the pollutant distribution.

2c. *Methodology*

In the present study, the ARW mesoscale atmospheric model and the HYSPLIT dispersion model were integrated to identify the sources using backward trajectories and then computing the dispersion of pollutant from the source location. As the first step, time series of hourly values of Mercury species available from NOAA NERR observation station located on the Mississippi Gulf Coast (30.41N, 88.4W) were examined and an episode of maximum in the observations was identified and taken up as case study. The second step was to run the ARW model at 4 km resolution, covering the Mississippi Gulf Coast region, for 48 hours starting from 24 hours prior to the chosen time related to observed maximum. HYSPLIT model was run, driven by the simulated atmospheric flow fields, to produce the back trajectories of parcels originating from the observation location. The mixing depth required for back trajectory calculation are taken from the meteorological model simulations. These back trajectories provide the Lagrangian path of the air parcels that could have contributed for the observed peak value at the observation site. The possible sources could be identified from the simple trajectory paths and matching them with the pollution sources identified by Mississippi Department of Environmental Quality(MDEQ) for the corresponding time period. Once the sources are identified, HYSPLIT model was run with hypothetical emission strengths to produce the spatial dispersion of the pollutant (RGM in the present study, for a 24 hour period). For the present study, emissions from four power plants which fall in the back trajectory path (Charles R Lowman power plant, Barry power plant in Alabama, Jack Watson power plant and Daniel power plant in Mississippi) were taken as sources and the atmospheric dispersion characteristics of the pollutant from these two sources were plotted and analyzed. In the forward model in HYSPLIT, the dispersion is treated with full 3-D particles in horizontal and vertical directions where the dispersion is computed by adding a random component to the particle motion. The vertical turbulent diffusion is treated using the Kantha and Clayson (2000) approach where the boundary layer velocity variances are defined as a function of the surface layer parameters and the mixing height. The horizontal turbulence is treated proportional to the vertical turbulence. The bondary layer stability functions are derived from heat and momentum fluxes using the meteorological model fields and the vertical mixing profile is treated to vary within the PBL.

3. RESULTS AND DISCUSSION

The time series of pollutant observations, available from NOAA NERR station located on Mississippi Gulf Coast (30.41N, 88.4W), were analyzed for the one month periods of May 2008 and an episode with a maximum of 75 pg/m3 was identified at 16 UTC of 5 May 2008. The reason for the selection of this episode was because of the very high RGM that was measured. The location of the NERR station along with emission sources around the study region is shown in Figure 2. The time-series graph of the measurements of mercury concentrations i.e., Reactive Gaseous Mercury (RGM), Gaseous Elemental Mercury (GEM), Fine Particulate Mercury (FPM) and also a time series graph of the trace gas concentrations measured at the site are presented in Figure 3. It shows variations of RGM, GEM during 00 UTC of 3 May to 00 UTC of 8 May 2008. These time series show relatively larger values of RGM during 5-6 May 2008 around 75-170 pg/m3. Though there is variation of GEM (1.4-1.6 ng/m3), but it is at a relatively lower level in comparison to that of RGM values. The RGM peaks are one of the highest that have been measured at the site. Though there is variation of GEM, it is a variation among relatively small values.

3.1 Simulated wind Flow and surface meteorological parameters

As mentioned in the preceding paragraph, a peak value of 75 pg/m3 of RGM was observed at NERR location at on 6 May, 2008. As per the adopted methodology, ARW mesoscale model was integrated for 48 hours starting from 00 UTC of 4 and 5 May to simulate the atmospheric fields at 4 km resolution as described in Section 2. These high resolution atmospheric fields were provided as input HYSPLIT model for computing back trajectories, source identification and spatial atmospheric dispersion characteristics. The ARW model derived atmospheric wind flow at 10m height over the study region corresponding to 00 UTC of 5 May 2008 is presented in Figure 4 along with the EDAS wind field. From the EDAS 40 km data the near surface wind circulation at 00 UTC 5 May is northerly in north Mississippi, northwesterly in south Mississippi , Gulfcoast and the oceanic region. The northwesterly wind field in Mississippi and at the coast gradually changes to

northeasterly at 12 UTC, and to northwesterly at 18 UTC. It becomes westerly in southern Mississippi and at the Gulf coast at 00 UTC 6 May. The ARW 36 km data shows northwest winds over northeast parts of the model domain (i.e.) eastern parts of the land where as the wind flow is very light in strength and mostly from north direction. The wind flow is stronger over southern ocean region with an approximate strength of 10 m/s and with the direction of flow as from north over eastern parts and northeast over western region. This shows the distinct variation in the strength between western and eastern parts and of the land and ocean regions of the model domain. The near surface wind flow adjacent to the coast has a diurnal flow pattern in both EDAS and ARW fields. The direction of the wind flow changes diurnally from west (00 UTC), north/ northwest (06, 12 UTC) and northeast (18 UTC) respectively in all the cases at the coast. Over the land region though there is no pronounced shift in wind direction a slight diurnal change in wind from northwest, north and northeast could be noted and it is more prominent in the higher resolution ARW data.

The ARW predicted near surface wind field from 36 km grid is not much different from the EDAS wind field uptill 5/18 UTC May. A few differences in wind field are identified at 5/18 UTC , when the EDAS has northwesterly winds in Mississippi while the ARW has northeasterly surface winds. Also at this time the wind field from ARW is divergent in Louisiana in contrast to the easterly winds found in EDAS. The main difference in the EDAS and ARW fields is the ARW shows a slight sea breeze component (southwesterly winds) at the coast between 12 UTC and 18 UTC and is more conspicuously noted in the high resolution (4 km domain) simulation. The surface horizontal winds are slightly stronger in the ARW simulations especially from the 4 km inner domain simulations than in the EDAS data. In both the EDAS and ARW model data the vertical winds are positive (upward motion) during the convective day time conditions and slightly negative (downward motion) in the stable night conditions. The 4 km ARW winds from the inner domain indicate positive vertical winds adjacent to the coast (1-4 cms^{-1}) and negative vertical winds in the northeastern and central parts of the land region. The vertical winds (both positive and negative) are relatively stronger in the ARW data especially from its 4 km resolution grid. The surface temperature is an indicator of the surface turbulent heat flux and is noted to be higher by about 2°C in the EDAS data than in the ARW data.

3.2 Simulated Back trajectories

The Hysplit model simulated Lagrangian back trajectories for the 48 hour period ending at 06 May 08 in respect of meteorological fields from EDAS 40 km, ARW 36 km and ARW 4km grid simulations are shown in Figure 5. The HYSPLIT model was run to produce 24-hour length back trajectories during 00 UTC of 4 May to 00 UTC of 6 May 2008 with the NERR monitoring site as the source point. The back trajectories are calculated at every 1-hour interval from ARW data (due to its high temporal resolution) which yielded 48 back trajectories for the ARW cases and at every 3-hour interval from EDAS data which yielded 16 back trajectories for the EDAS case. The computed back trajectories at 00 UTC of 6 May 2008 (Figure 5) show that the air parcels are from North of Northwest to North culminating at the NERR location and the height of the parcels to be below 1500 m level.

It is seen that the trajectories are differently simulated in these three cases. Most of the trajectories from ARW 36 km data are oriented from northwest/ northeast to NERR with the air parcels coming from northeastern parts of Mississippi and western parts of Alabama through the source locations Lowman, Barry and Daniel power plants. A few trajectories are oriented from northeast / northwest to NERR with the air parcels coming from the central and eastern parts of the Mississippi through the source locations Eaton and Daniel power plants. The trajectories from the EDAS fields are mostly oriented in northwest to south passing thorough the source points at Lowman, Daniel and Eaton. A few trajectories of very short time length (about 6 hours) are noted both from EDAS and ARW data sets to reach from southeast from the ocean and they indicate the ariparcels passing through the source points Watson and Pascagoula MSW (waste incineration plant). These onshore trajectories from ocean are more prominently seen in the ARW cases. The EDAS trajectories are relatively well separated compared to the ARW trajectories probably because the latter are calculated at 1 h interval and hence denser in frequency. The main difference is the trajectories from ARW data traveled relatively from farther ranges because of relatively higher wind speeds in ARW data and covered larger number of Hg sources along the mean path. The trajectories computed from ARW 4 km data are distinctly different in that most of them are aligned from northeastern direction extending to far western Alabama and a few have originated from northwest and west directions in Mississippi. With this eastward spread, the trajectories from ARW 4 km data completely covered the sources of coal fired power plants at Eaton in Hattisberg, Daniel, Watson along the MS Gulf coast and the sources Lowman, Barry in Louisiana. Among these sources only one or two trajectories pass along the source Eaton in both the EDAS and ARW cases. Yet another important difference is that the EDAS trajectories throughout the 48 hour period are confined to the surface level (10 m AGL) while those from ARW simulations rise vertically after the first 18 hours of simulation thus allowing the vertical mixing of air parcels in the upper atmospheric regions. While the trajectories from ARW 36 km data rise up to 800 m AGL those from ARW 4km fields are noted to rise upto 1500 m AGL. The trajectories in ARW 4 km data also exhibit the diurnal cycle of vertical movement of trajectories in the lower atmosphere upto 1500 m AGL. This clearly indicates the role of the boundary layer turbulence, thermal convection and the resulting vertical motion field on the simulated trajectories with the mesoscale meteorological fields obtained from ARW 4 km simulations.

Thus the simple back trajectory analysis indicates a few differences in the trajectories computed from the coarse EDAS data and high resolution ARW 4 km data. The trajectories from ARW 4 km data seem to be more eastward and realistic as they account for the air parcel motions under the expected mesoscale circulations and associated turbulence and vertical motion fields in the coastal region. The mean trajectory paths indicate four important sources of Hg i.e.., Charles R Lowman Power Plant, located at 31.489N, 87.9W, Barry Power plant located at 30.84N, 88.09W in Alabama State and Jack Watson Power Plant located at 30.44N, 89.026W, Daniel power plant located at 30.64N, 88.59W in Mississippi State. Since the emission strength of different mercury species (RGM, GEM, FPM) at these sources is not known, a hypothetical emission strength of RGM was taken as 1.0 g/h for the dispersion computations.

3.3 Forward Dispersion Simulations

With this input to HYSPLIT model, forward dispersions were computed originating from these four sources. The HYSPLIT produced 24 hour ground level (0-25 m AGL) RGM concentration patterns are presented in Figs 6 and 7 corresponding to the EDAS coarse data and the high resolution ARW 4km meteorological data sets respectively. The plume distribution from Lowman Power Plant (Figure 6a) was oriented towards south and within an arc distance of 20-30 degrees indicating a narrow region and contributing high concentration (about 10^{-13} g/m3) to the NERR location. The plume from Lowman corresponding to ARW fields is oriented towards southeast and has a wider spread with an arc distance of 40 degrees and contributing a concentration between 10^{-13} and 10^{-15} g/m3 which may be due to higher wind strength with ARW data. The plume from Watson power plant (MS) with EDAS data is distributed towards south and southwest from the source location (Fig 6b) and has a relatively higher spread (with an arc angle of 30-50 degrees) than that at Lowman. From this location of Watson Power Plant, the plume covers nearly double the ground area confined to a narrow region in the westward direction and also the plume quickly disperses to two orders less concentration in the downwind region. It just hits the NERR site wit a very minute concentration of about 10^{-17} g/m3. The plume computed from the Watson location with the ARW data is distributed to the west and southwest from the source location (Fig 7b) and does not cover the NERR site and it is less dispersed in the downwind region than in the case of EDAS data.

The plume distribution from the Daniel plant location using the EDAS fields (Fig 6c) is oriented in the southeast direction with arc length of 60 to 120 degrees. The plume region near the source with a concentration range of 10^{-12}-10^{-14} g/m3 covers the NERR site. The plume with the ARW data from the Daniel plant location is mostly distributed to the west and southwest quadrants (Fig.7c) and does not cover the NERR site as it is in the plume upwind region for this case. The plume distribution pattern for the Barry plant location using the EDAS fields (Fig.6d) is oriented in the southwest and south directions from the source and is relatively less spread than for the Watson and Daniel plant plumes. The plume for this source from EDAS fields is not spread much along the coast and hence does not cover the NERR site. The dispersion for the Barry plant source computed with the ARW fields indicates the plume is spread predominantly in the southwest direction and completely covers the NERR site with a high concentration. Mention must be made here that the plume distribution pattern discussed above is for the whole 24 hours period from 00 UTC 05 May to 00 UTC 06 May and it does not represent the plume positions at various hours. The plume residence time at different instances actually varies during the 24 hours period. Hence the diurnal time series of concentration simulated at the NERR site due to each of the sources in each case (EDAS and ARW) varies according to whether there is incidence of the plume and its residence time which is more clearly discussed below.

The time series of the ground level plume concentration at the NERR site from the four sources for the forward dispersion simulations using EDAS and ARW data are shown in figure 8 along with the time series of the RGM concentrations at the NERR site on the right y-axis. Since dispersion simulations are made with hypothetical release strength of RGM at each of the four sources the purpose is not to compare the model values with the absolute measured concentration levels but to compare the occurrence of relative peaks in concentrations from different sources. From the time series plot in respect of the calculations with EDAS data it is found that two sources namely Lowman and Daniel contribute to the peak concentrations at NERR site, the contribution from Daniel is roughly 9 hours before and the contribution from Lowman is roughly 5 hours later than the occurrence of the peak in the measured concentration at NERR (Fig 8a). The highest contribution is from Lowman plant followed by the Daniel plant. In the case of the calculation with ARW 4 km data set the time series plot indicates two sources namely Lowman and Barry chiefly contribute for the high concentration levels at NERR (Fig 8b). It also shows multiple peaks in concentration at different times during the day from these two sources. The highest concentration is contributed by the Barry plant followed by Lowman roughly about 4 hours before the actual peak in measured concentration. The second peak in concentration occurred at roughly 6 hours and 8 hours later than in the measured concentration from the Barry and Lowman locations respectively. Of the four sources Watson is to the west of the monitoring site and the wind circulation during most of the day is northerly and northeasterly, hence the plume from Watson did not hit considerably the monitoring station during the study period, leading to no significant model concentration from either EDAS and ARW fields. The source Barry located on the southwestern Alabama is farther than the source Daniel (about 20 km away) from NERR. However, the contribution from the source Daniel is not significant in the simulation with ARW data mainly because of the plume incidence from southwesterly

direction on the NERR site and because the NERR is located on the upwind region from Daniel source. Thus the representation of the wind field in the EDAS and the ARW data caused major differences in the transport of the RGM from these two nearby sources in the two simulations. The multiple peaks in the simulated concentrations using ARW data is due to the diurnal circulation at the coast found in the ARW simulations indicating the impact of the sea- land breeze type mesoscale phenomena causing frequent plume transitions.

4. Summary and conclusions

This study demonstrates the application of integrated weather prediction and atmospheric dispersion models to identify the sources of a pollutant. This involves computing back trajectories from the observation location using HYSPLIT dispersion model driven by high resolution meteorological fields produced by ARW model. As a continuation of this study, hourly values are being analyzed to identify the peak hour emissions during a particular day, such as 5-6 May 2008 episode and then draw the back trajectories from that particular hour to identify the source(s) that could have contributed for a particular hourly high value. Inorder to account for the contributions from different sources to the observed values of RGM at NERR simulations are conducted using both coarse scale EDAS meteorological data and the high resolution meteorological data simulated using ARW model.

The simulations using EDAS and ARW data reveal that the sources Lowman, Daniel and Barry are likely to contribute to the observations at NERR location during study period. As Lowman Power Plant is situated far away about 200-300 km from NERR location, its contribution as noted from the simulation with EDAS data is doubtful as it has a very coarse scale representation of the wind field (both in terms of strength and direction) and the wind trajectories are confined in the shallow lower atmospheric region throughout the 48 hours period due to poor representation of the vertical wind component in the EDAS data. Similarly the contribution from Daniel plant in the case of the simulation with EDAS data is because of the steady wind flow from north over the upwind land region causing the plume to spread in the south direction and hitting the NERR site. In contrary to this flow pattern, the ARW wind field adjacent to the coast appears more dynamic with diurnal wind shifts causing the plume to spread significantly to the southwest and also to some extent to the south. As the plume in the case of EDAS data for the source Barry was mostly from north and less lateral dispersion adjacent to the coast it did not contribute much to the NERR site, while the simulated plume in the case of ARW data has large lateral dispersion adjacent to the coast and covered the NERR site. The wide dispersion near the coast noted in the simulation with ARW data is because of the inhomogenity in the wind field across the coast arising due to the onset of the sea breeze and its interaction with the flow field inland. This leads to the alteration in the atmospheric mixing region across the coast and the associated, temperature, humidity and turbulence characteristics. This phenomena is commonly observed at many coastal regions and is attributed to the cause for fumigation. The wind field and other meteorological fields from the fine scale ARW simulations at the Mississippi Gulf coast are compared with observations in earlier studies and the sea breeze is confirmed with experimental observations. Thus the back trajectories and plume dispersion pattern simulated with ARW fine scale meteorological fields appear to be more realistic than those computed with the coarse EDAS data. From the dispersion spread of emissions (using WRF-HYSPIT) from a number of sources surrounding the NERR site, two power plants (Charles R Lowman power plant and Barry power plant in Alabama) which fall in the back trajectory path are found to most likely to significantly contribute to the observations at NERR location during episode period studied. The advantages of HYSPLIT model to produce the forward time dispersion of the pollutant (mercury in this study) is also demonstrated through this study.

5. ACKNOWLEDGMENT

This study is carried out as part of the ongoing Atmospheric Dispersion project (ADP) funded by National Oceanic and Atmospheric Administration (NOAA) through the U.S. Department of Commerce Grant #NA06OAR4600192.

6. REFERENCES

Anjaneyulu, Y., C. V.Srinivas, I. D., Jayakumar, J. Hariprasad, J. Baham, C. Patrick, J. Young, Hughes, L. D., White, M. G. Hardy and S. Swanier. Some observational and modeling studies of the coastal atmospheric boundary layer at Mississippi Gulf coast for Air Pollution Dispersion assessment: *Int. J. Environ. Res. Public Health*, 2008, *5(5)* 484-497.

Anjaneyulu, Y., C. V. Srinivas, H. P. Dasari, L. D. White, J. M. Baham, J. H. Young, R. Hughes, C. Patrick, M. G. Hardy and S. J. Swanier. Simulation of Atmospheric Dispersion of Air-Borne Effluent Releases from Point Sources in Mississippi Gulf Coast with Different Meteorological Data. *Int. J. Environ. Res. Public Health*, **2009,** *6*, 1055-1074.

Challa, Venkatasrinivas, Jayakumar Indracanti, J. M Baham, R. Hughes, C. Patrick, J. Young, M. Rabbarison, S. Swanier, M. G. Hardy and Y. Anjaneyulu. Sensitivity of Atmospheric dispersion simulations by HYSPLIT to the meteorological predictions from a mesoscale model *Environ. Fluid Mechanics*, **2008**, 8:367-387.

Challa, Venkatasrinivas, Jayakumar Indracanti, J. M Baham, R. Hughes, C. Patrick, J. Young, M. Rabbarison, S. Swanier, M. G. Hardy and Y. Anjaneyulu**.** A Simulation Study of Meso-Scale Coastal

Circulations in Mississippi Gulf coast for Atmospheric Dispersion. *Atmos. Res., **2009**,* 91, 9-25.

Draxler, R.R.; Hess, G.D. An overview of the HYSPLIT_4 modeling system for trajectories, dispersion and deposition. *Australian Meteorological Magazine* **1998**, 47, 295-308.

Dudhia, J., Numerical study of convection observed during winter monsoon experiment using a mesoscale two-dimensional model. J. Atmos. Sci. **1989.**, 46, 3077–3107

Dudhia, J., A multi-layer soil temperature model for MM5, Preprint from the Sixth PSU/NCAR Mesoscale Model Users' Workshop, **1996.**

Hong, S. Y., Noh, Y., Dudhia, J., A new vertical diffusion package with explicit treatment of entrainment processes. Mon.Wea. Rev. **2006**, 134, 2318-2341.

Jin, H.; Raman, S. Dispersion of an Elevated Release in a Coastal Region. *J. Appl. Meteor.***1996**, 35, 1611–1624.

Kain, J. S., Fritsch, J. M., Convective parameterization for mesoscale models: The Kain-Fritcsh scheme, The representation of cumulus convection in numerical models. K. A. Emanuel and D.J. Raymond, Eds., Amer. Meteor. Soc., 246 pp, **1993.**

Kantha, L.H. and C.A. Clayson, Small Scale Processes in Geophysical Fluid Flows, International Geophysics Series, Academic Press, San Diego, **2000,** 67, 883 pp.
Kotroni, V.; Kallos, G.; Lagouvardos, K.; Varinou, M. Numerical simulations of the meteorological and dispersion conditions during an air pollution episode over Anthes, Greece. J. Appl. Meteor. **1999**, 38, 432-447.

Lu, R.; Turco, R.P. Air Pollutant transport in a coastal environment II. Three-dimensional simulations over Los Angeles Basin. *Atmos. Env*. **1995,** *29*, 499-1518.

Mlawer, E. J., Taubman, S. J., Brown, P. D., Iacono, M. J., Clough, S. A., Radiative transfer for inhomogeneous atmosphere: RRTM, a validated correlated-k model for the longwave. J. Geophys. Res. **1997**, 102 (D14), 16663–16682.

Moran, M. D.; Pielke, R. A., Sr. Evaluation of a mesoscale atmospheric dispersion modeling system with observations from the 1980 Great Plains mesoscale tracer field experiment. Part II: Dispersion simulations. *J. Appl. Meteor.* **1996**, 35, 308-329.

Pacific Environmental Sciences Inc Vol.IX, Chapter 1:Emission Inventory methods for $P.M_{2.5}$, **1999.**

Physick, W.L.; Abbs, D.J. 1991. Modeling of Summertime Flow and Dispersion in the Coastal Terrain of Southeastern Australia. Mon. Wea. Rev. **1991**, 119, 1014-1030.

Pielke. R.A.; Lyons, W.Y.; McNider, R.T.; Moran, M.D.; Moon, D.A.; Stocker, R.A.; Walko, R.L.; and Uliasz, M. Regional and Mesoscale meteorological modeling as applied to air quality studies. In *Air Pollution Modeling and its Application* VIII., H.van Dop, and D.G.Steyn, Eds., Plenum Press, New York, USA, **1991**, 259-289.

Segal, M.; Pielke, R.A.; Arritt, R.W.; Moran, M.D.; Yu, C.H.; and Henderson, D. Application of a mesoscale atmospheric dispersion modeling system to the estimation of SO_2 concentrations from major elevated sources in southern Florida. Atmos. Env. **1988**, 22(7), 1319-1334.

Skamarock, W.C.; Klemp, J.; Dudhia, J.; Gill, D.O.; Barker.; D.M., Wang, W.; Powers, J.G. A Description of the Advanced Research WRF Version 2. NCAR Technical Note, NCAR/TN-468+STR. Mesoscale and Microscale Meteorology Division, National Center for Atmospheric Research, Boulder, Colorado, USA. **2005.**

Wang, G.; Ostoja-Starzewski, M. A numerical study of plume dispersion motivated by a mesoscale atmospheric flow over a complex terrain. *Appl. Math. Model* **2004**, 28, 957-981.

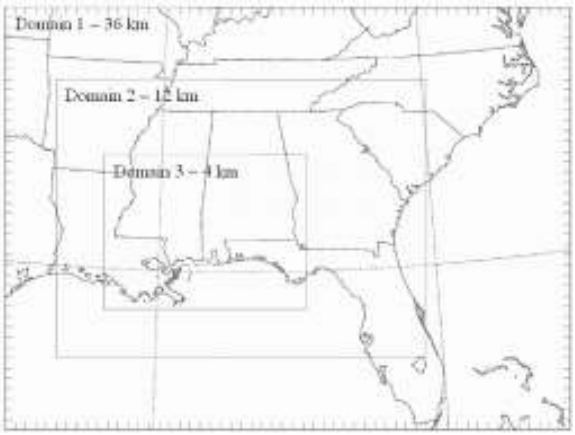

Figure 1. Model domains

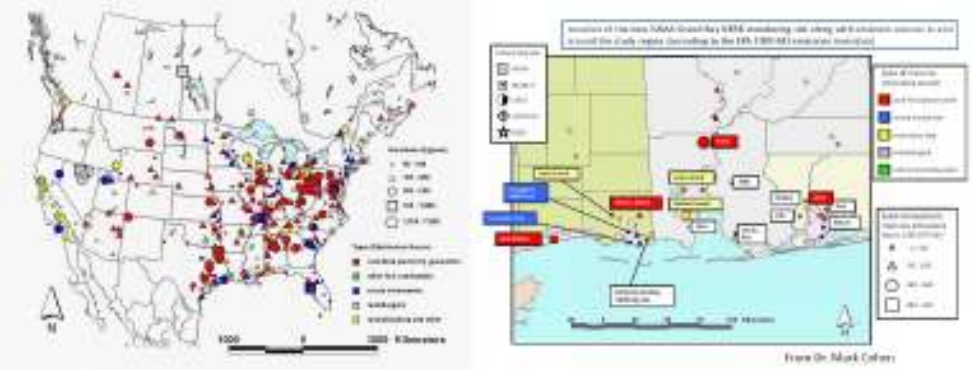

Figure 2. Locations of pollutant sources over USA (left) and Gulf Coast region (right)

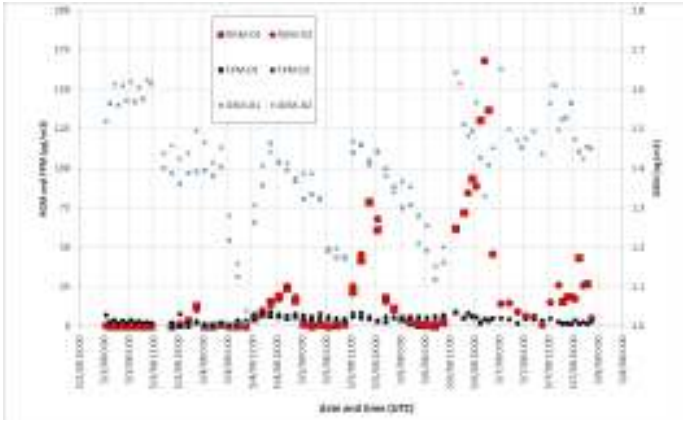

Figure 3. Time series of Mercury emissions at NERR Grand Bay Location

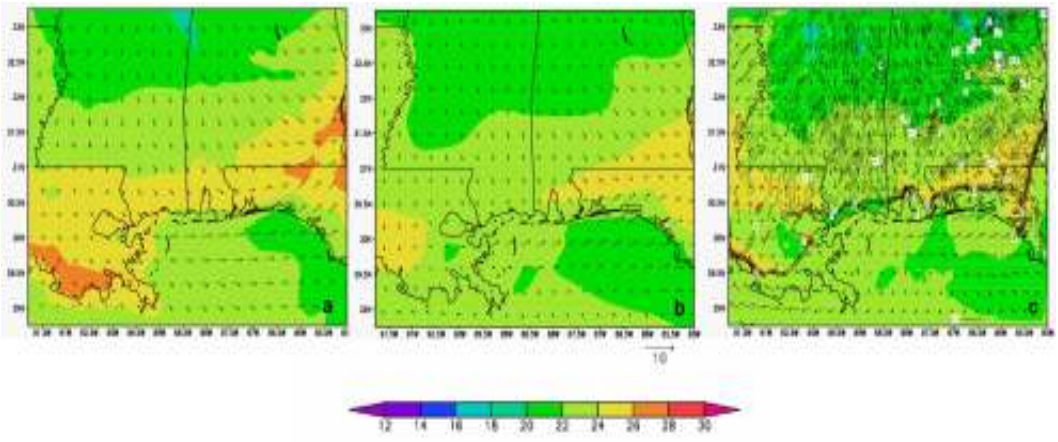

Figure 4. Spatial distribution of wind and temperature over the study region as derived from EDAS-40 km (left); ARW-36km (middle) and ARW-4 km (right)

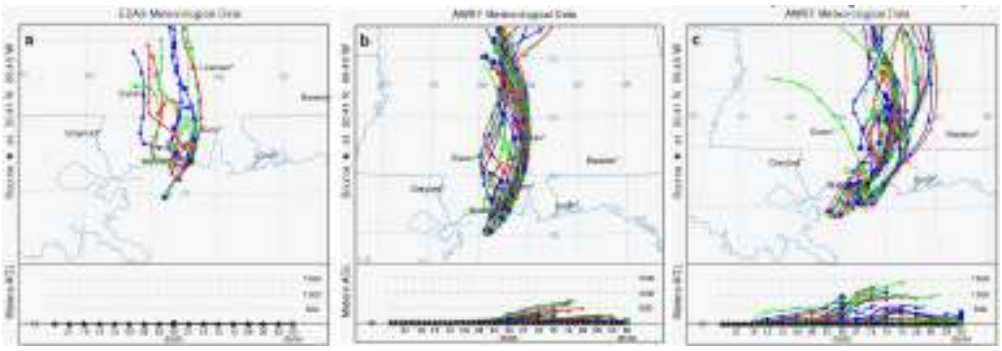

Figure 5. Back trajectories produced by HYSPLIT model using EDAS-40 km (left); ARW-36km (middle) and ARW-4 km (right)

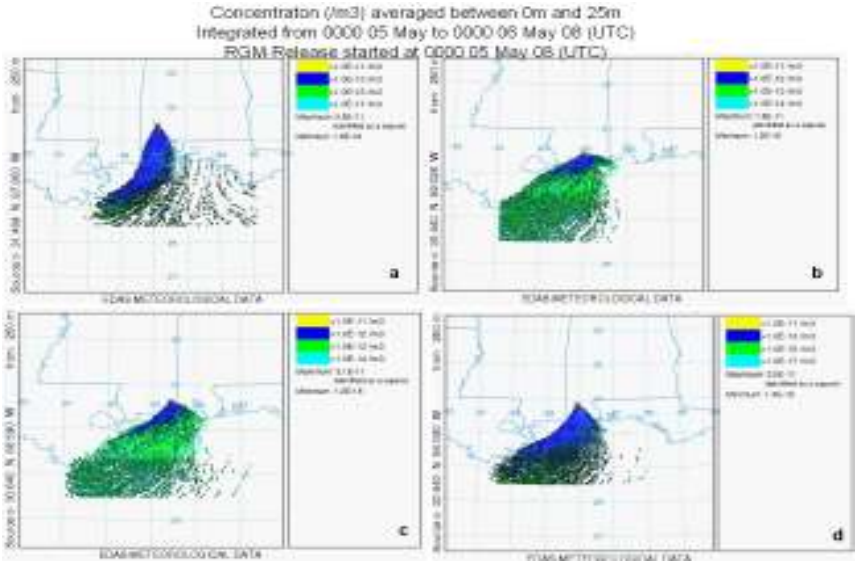

Figure 6. Atmospheric dispersion as predicted by HYSPLIT model using EDAS-40 km data from the four different sources of Lowman (upper left) , Watson (upper right) , Daniel (bottom left) and Barry (bottom right)

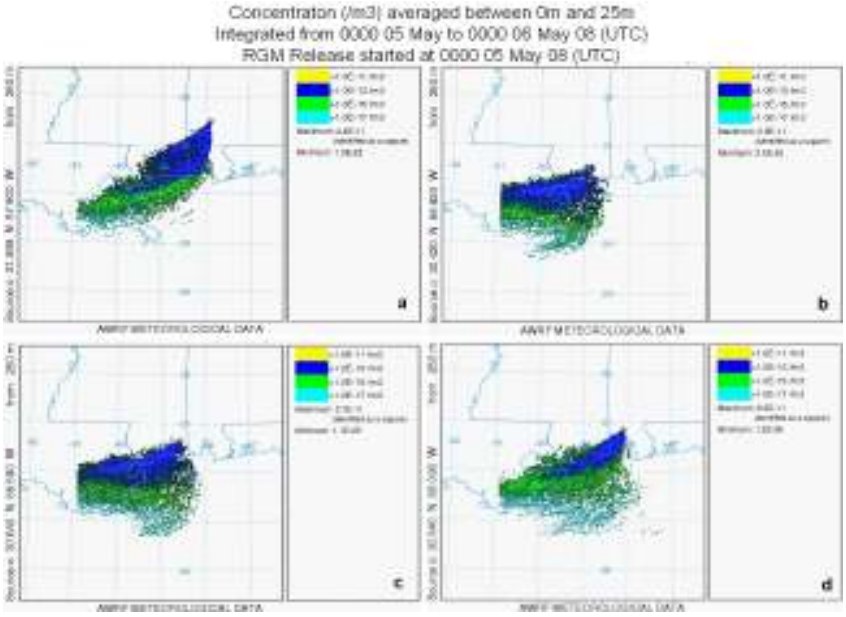

Figure 7. Atmospheric dispersion as predicted by HYSPLIT model using ARW- 4 km data from the four different sources of Lowman (upper left) , Watson (upper right) , Daniel (bottom left) and Barry (bottom right)

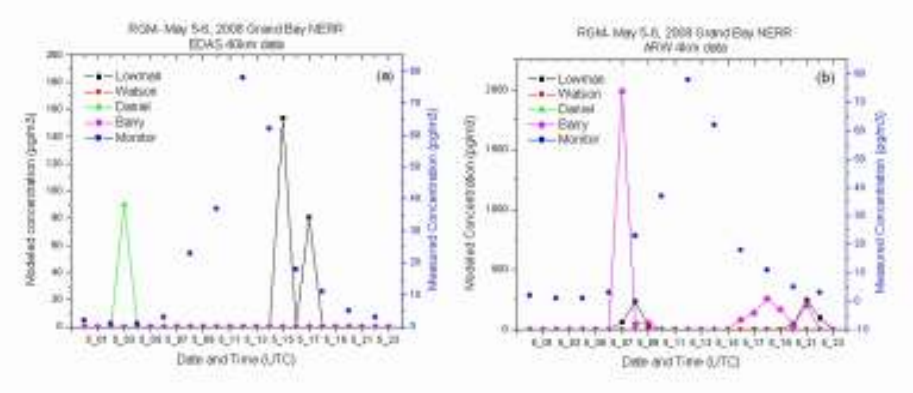

Figure 8. Trends in the simulated and measured RGM concentrations as produced from EDAS-40km and ARW-4 km data.